



# Identification of Micro-plastics (MPs) in Conventional Tap Water Sourced from Thailand

Dinuka Kankanige & Sandhya Babel\*

School of Bio-Chemical Engineering & Technology, Sirindhorn International Institute of Technology, Thammasat University, Khlong Luang, Pathum Thani 121210, Thailand

\*E-mail: sandhya@siit.tu.ac.th

## Highlights:

- 6.5-53  $\mu\text{m}$  MPs were dominant ( $56 \pm 14$  p/L) in all the tap water samples tested.
- Fibers dominated (58%), followed by fragments (37%) and films (5%).
- Major polymers detected for  $\geq 300$   $\mu\text{m}$  particles: PE, PVC, PET, PA, PTFE, PP, and PAM.
- Ingestion of smaller-sized MPs by humans, especially fibers, causes potential health risk as there may be cellular uptake.

**Abstract.** In a period when MP contamination of drinking water is a great concern, this study focused on the size- and morphology-based count, and polymeric identification of plastic particles in tap water sourced from Thailand. A total of 45 human consumable samples (each 1 L) were collected at Thammasat University. The average MP counts sorted by Nile Red tagging were  $56.0 \pm 14.0$  p/L (6.5-53  $\mu\text{m}$ ) and  $21.0 \pm 7.0$  p/L (53-300  $\mu\text{m}$ ), while those found by optical microscopic observations were  $13.0 \pm 5.0$  p/L (300-500  $\mu\text{m}$ ) and  $6.0 \pm 3.0$  p/L ( $\geq 500$   $\mu\text{m}$ ). A significantly high MP amount was observed in the 6.5-53  $\mu\text{m}$  fraction. Fibers dominated in all samples, accounting for 58% of the particle count. Most  $\geq 300$   $\mu\text{m}$  particles tested by ATR-FT-IR spectroscopy were confirmed to be polymeric, identified as PE, PVC, PET, PA, PTFE, PP, and PAM. These particles may have escaped from the treatment plant or were added along the water distribution network. Since MPs in drinking water constitute a potential health risk by exposing humans to direct plastics intake, MP contamination in water supply systems should be controlled.

**Keywords:** *ATR-FT-IR spectroscopy; micro-plastics (MPs); Nile Red; optical microscope; tap water.*

## 1 Introduction

MP contamination of aquatic systems is a serious environmental issue that leads to chemical and ecological hazards (Li, *et al.* [1], GESAMP [2]). Water bodies are largely MP-contaminated due to mismanaged plastic debris disposal and through wastewater discharge (Ziajahromi, *et al.* [3]). MPs are also found in drinking water sources, which is an emerging concern in this field. Investigating

MPs in tap water is required to understand their pathways in the water supply system. Moreover, consumption of MP-contaminated drinking water exposes humans to direct and long-term plastic intake (Li, *et al.* [1]). Investigations on this matter have been conducted in Europe and the United States, but not in the Asian and African regions.

Providing potable water is a worldwide challenge. Knowing the size- and morphology-based contamination levels of MPs in human-consumable water is important due to their size- and shape-dependent toxicity. Kosuth, *et al.* [4] reported anthropogenic particles in 81% of 159 globally sourced tap water samples with an average of 5.45 p/L in the 0.1-5 mm fraction. The current study analyzed  $\geq 6.5 \mu\text{m}$  plastics in tap water from Thailand and quantified the MPs, focusing on smaller-sized particles.

The analysis was based on fluorescent tagging with Nile Red (6.5-300  $\mu\text{m}$ ) and optical microscopic observations, followed by ATR-FT-IR spectroscopy ( $\geq 300 \mu\text{m}$ ). The study had two objectives: 1) counting the  $\geq 6.5 \mu\text{m}$  MPs based on size and morphology; 2) identification of the polymer types among the sorted  $\geq 300 \mu\text{m}$  particles. The findings are helpful in informing the public and authorities of the status of MP contamination in municipal drinking water in Thailand and should prompt relevant parties to take action for minimizing the contamination level.

## 2 Methodology

### 2.1 Sample Collection

Tap water, distributed along PVC pipelines, was collected from 5 locations at Thammasat University on 5 sampling days in April 2019. At each location, 3 samples (1 L each) were collected at 6-hour intervals in triplicate. Accordingly, 9 L of tap water was collected per location, so the total sample volume was 45 L. A tap was kept open and water was allowed to flow for 1 minute. A bottle (DURAN<sup>TM</sup> clear glass laboratory bottle) was rinsed thrice with tap water and then filled with tap water, after which the opening was wrapped with aluminum foil and capped tightly.

Aluminum foil was used to avoid the plastic contamination that could occur by the contact between the polypropylene screw cap and the sample. The samples were stored in a refrigerator at 4 °C until processing to avoid thermal impact. Samples from each sampling event were processed within 24 hours after storage. Table 1 summarizes the details of the sampling events performed at each location.

**Table 1** Sampling events at Thammasat University (Rangsit campus), Thailand.

Location	Purpose	Sampling events per day		
		1 (07:00)	2 (13:00)	3 (19:00)
Green canteen (L <sub>1</sub> )	Drinking/cooking	1 L × 3	1 L × 3	1 L × 3
TU hospital (L <sub>2</sub> )	Drinking/cooking	1 L × 3	1 L × 3	1 L × 3
SIIT canteen (L <sub>3</sub> )	Drinking/cooking	1 L × 3	1 L × 3	1 L × 3
TSE canteen (L <sub>4</sub> )	Drinking/cooking	1 L × 3	1 L × 3	1 L × 3
SC canteen (L <sub>5</sub> )	Drinking/cooking	1 L × 3	1 L × 3	1 L × 3

## 2.2 Filtration, Size Fractionation, and Nile Red Staining

The samples were filtered through 500 µm, 300 µm, 53 µm sieves, and 0.45 µm cellulose nitrate membrane filters (Sartorius Stedim Biotech GmbH, Germany, 45 mm). Accordingly, they were fractionated into 4 size categories: ≥ 500 µm, 300-500 µm, 53-300 µm, and 6.5-53 µm. Residue on the 500 µm and 300 µm sieves was rinsed off with deionized water, reconstituted into beakers, vacuum filtered through a 0.45 µm gridded membrane filter, and dried at room temperature. The remaining samples for the 53 µm sieve and 0.45 µm membrane filters were similarly rinsed off with deionized water and reconstituted into 100-150 mL samples for subsequent staining with Nile Red dye.

The method of Nile Red tagging was conducted as per Maes, *et al.* [5]. Nile Red (Nile Blue a Oxazone, Sigma Aldrich, GmbH, Germany) fluorescent dye was dissolved in methanol (PGII, Ajax Finechem, Thermo Fisher Scientific, NZ) to prepare a 1 mg/mL of stock solution. The stock solution was injected into each sample to get a working concentration of 10 µg/mL. After incubating the samples at 30 °C for 30 minutes, they were vacuum filtered through the same filters used for optical microscopy, and dried at room temperature prior to analysis.

## 2.3 Enumeration

Visual sorting using an optical microscope (Olympus CX41, Philippines) was employed for the 300-500 µm and ≥ 500 µm fractions. Particles were observed under a 4× to 40× objective and 10× eyepiece, counted, and sorted according to morphology (fibers, fragments, and films). Nile Red stained filters of 6.5-53 µm and 53-300 µm were each divided into 4 equal segments of 12 × 12 mm<sup>2</sup> to represent 4 quadrants of the filter, and scanned segment-wise by a fluorescence microscope (GE Healthcare, Delta Vision Elite, USA) under a 4× to 20× objective and 10× eyepiece. A DAPI (4', 6-diamidino-2-phenylindole) filter was used to detect the Nile Red tagged particles that clearly fluoresced in blue against a dark field (excitation: 390/18 nm, emission: 435/48nm).

Nile Red shows a preferential adsorption for polymeric particles relative to common organic and inorganic environmental contaminants (Maes, *et al.* [5]).

This method of Nile Red staining has been validated by FT-IR analysis to verify the polymeric content of the fluorescing particles (Erni-Cassola, *et al.* [6]). As per this latest evidence, Nile Red can be used for rapid detection of smaller-sized MPs in tap water. Based on the pixel size that could be imaged under the lowest magnification (4× objective), the lower size boundary of the particles was set to 6.5  $\mu\text{m}$ . Each scanned segment was analyzed by the ImageJ software (version 1.52n) to count the number of particles and sort the particles into fibers, fragments, and films. The segment-based particle count was totaled for the whole filtered area. All quantified results are presented as particles per liter (p/L).

#### **2.4 ATR-FTIR Analysis of $\geq 300 \mu\text{m}$ Particles**

For polymer-identification, specimens from the 300-500  $\mu\text{m}$  and  $\geq 500 \mu\text{m}$  fractions were hand-picked and analyzed by ATR-FT-IR spectroscopy (Nicolet iS50, Thermo Fisher Scientific, USA) in the 400-4000  $\text{cm}^{-1}$  spectral range at 8  $\text{cm}^{-1}$  resolution for 128 scans. The background data were collected before every sample spectrum. The number of particles analyzed varied among the filters, depending on the feasibility of manually picking and transferring the particles onto the specimen-holder of the spectrometer.

Unknown spectra of the specimens were interpreted by comparison against the critical vibrational bands of the reference spectra and database matches in OMNIC 8.0 (HR Hummel Polymers & Additives,  $\geq 0.60$  match factor). Because most of the particles in the 53-300  $\mu\text{m}$  filters were not extractable and because of the analytical limits of the ATR-FT-IR spectrometer, spectroscopic confirmation was not applied for the 6.5-300  $\mu\text{m}$  particles. Nile Red adsorption was used for the primary indication of the polymeric nature of those particles (Mason *et al.* [7]).

#### **2.5 Steps to Minimize and Control Background Contamination**

All samples were processed inside a fume hood with laminar airflow to minimize contamination by environmental fibers. Sieves, glassware, and other tools were cleaned with 50% ethanol (v/v, (de-ionized water)/(absolute ethanol > 99.8%), RCI Labscan limited) and rinsed with de-ionized water prior to usage. Immediately before every filtration step, the blank filter papers were observed through an optical microscope to ensure that they were free of contamination. Powder-free non-latex nitrile gloves and a laboratory cloak were worn during sample handling and analysis.

For the quality control of the real samples, lab-blanks of de-ionized water were analyzed in triplicate for each sample set. One sample set refers to a group of samples collected from one location. De-ionized water was put into the same 1-L glass bottles at the sampling point itself, brought to the laboratory, stored, and

treated the same as the real samples. Since the samples were analyzed in 5 sets, 15 lab-blanks were processed. If MPs were detected in the lab-blanks, a correction for background contamination was applied to the final particle count in the corresponding real samples.

### 3 Results and Discussion

#### 3.1 Microscopic Observations

Figure 1 displays microscopic images of the MPs in the 300-500  $\mu\text{m}$  and  $\geq 500$   $\mu\text{m}$  fractions, observed under an optical microscope, showing particles of several shapes (fibers, fragments, and films). As per Rocha-Santos & Duarte [8], fragments were defined as particles with a rounded, sub-rounded, angular, or sub-angular shape. Films were defined as irregular-shaped (but thin) with mostly transparent particles, as reported by Zhou, *et al.* [9]. Different colored particles, such as blue, red, white, and transparent particles, were commonly noted. Particle color is a property that can be linked to a polymeric nature (Rocha-Santos & Duarte [8]) or additives that can leach from the MPs (Obmann, *et al.* [10]).

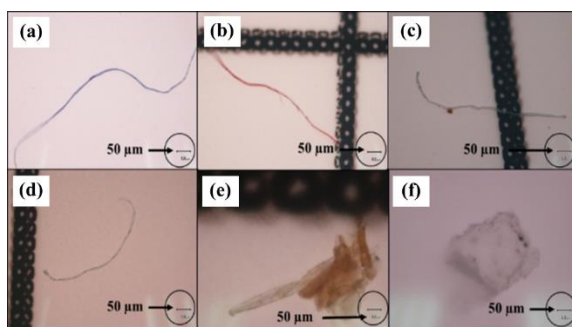


**Figure 1** Microscopic views of MPs observed under Olympus CX41 (10 $\times$  eyepiece, 10 $\times$  objective, scale bar = 50  $\mu\text{m}$ ): a) blue fiber; b) red fiber; c) and d) transparent fiber; e) brownish-transparent fragment; f) transparent film.

Images of blue-fluorescent particles under the fluorescence microscope are shown in Figure 2. These particles were in the range of 6.5-300  $\mu\text{m}$  and could not be effectively differentiated for morphology when observed under an optical microscope. Observations of the selected major polymer types under red (excitation: 542/27 nm, emission: 597/45 nm, TRITC (Tetramethylrhodamine) filter) and green (excitation: 475/28 nm, emission: 525/48 nm, FITC (Fluorescein isothiocyanate) filter) fluorescence, were largely influenced by background staining. Moreover, most of the polymers had a low fluorescent intensity, which disturbed clear particle visualization. Thus, blue fluorescence, which had a minimal background signal and generated a higher fluorescent intensity of the

major polymer types, was selected over red and green. The optical microscopic method with fluorescent tagging resulted in more convenient identification and counting of MPs.

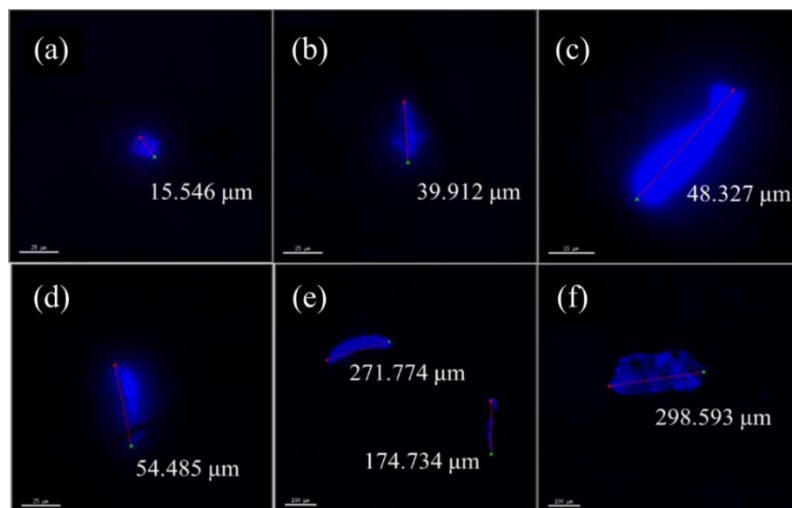


**Figure 2** Blue-fluorescent particles observed under DV Elite (DAPI filter, excitation: 390/18 nm, emission: 435/48 nm): a) fragment (200 $\times$ , scale bar = 25  $\mu\text{m}$ ); b) film (200 $\times$ , scale bar = 25  $\mu\text{m}$ ); c) fragment (40 $\times$ , scale bar = 15  $\mu\text{m}$ ); d) fiber (200 $\times$ , scale bar = 25  $\mu\text{m}$ ); e) fragment & fiber (40 $\times$ , scale bar = 100  $\mu\text{m}$ ); f) film (40 $\times$ , scale bar = 100  $\mu\text{m}$ ).

### 3.2 Background Contamination

Since MPs are ubiquitous in the environment, careful controls need to be in place during sampling, processing, and analysis. On average,  $9.0 \pm 3.0$  p/L,  $7.0 \pm 3.0$  p/L,  $4.0 \pm 3.0$  p/L, and  $2.0 \pm 1.0$  p/L were found for the following size fractions: 6.5-53  $\mu\text{m}$ , 53-300  $\mu\text{m}$ , 300-500  $\mu\text{m}$ , and  $\geq 500$   $\mu\text{m}$  respectively. Polyethylene (PE), polypropylene (PP), and polyamide (PA) were detected among the  $\geq 300$   $\mu\text{m}$  particles. These counts represent external contamination, occurring from the sampling point until the end of the analysis. MPs in the lab-blank collected during a particular event were deducted from the direct particle count of the real sample corresponding to that sampling event. Nile Red staining of the 6.5-53  $\mu\text{m}$  and 53-300  $\mu\text{m}$  particles involved a longer processing time than for the other samples, which only had to be filtered and stored for optical microscopic observation. As a consequence, the Nile Red stained samples were more exposed to environmental contamination than the other samples. Thus, when the time taken for sample processing and analysis was longer, it is reasonable to expect a higher background contamination in the real samples.

### 3.3 Size- and Morphology-based MP Count

Figure 3(a) shows the MP count in the tap water samples, averaged across the four size categories. Considering the 45 tap water samples analyzed, 6.5-53  $\mu\text{m}$  and 53-300  $\mu\text{m}$  MPs were found in the range of 24.0-85.0 p/L and 8.0-32.0 p/L, respectively. The sample values were 4.0-22.0 p/L for the 300-500  $\mu\text{m}$  fraction and 0-14.0 p/L for the  $\geq 500$   $\mu\text{m}$  fraction. The highest MP amount was reported for the 6.5-53  $\mu\text{m}$  fraction, which had a significantly higher mean ( $p < 0.05$ ) than the mean MP counts for the other size categories. This could be due to the fragmentation of larger particles into smaller ones. Figure 3(b) illustrates the morphology-based classification of the MP count for the four size categories. Fibers and fragments were the most commonly found particle shapes in all samples, while films accounted for the minority. In each size fraction considered, the mean for fibers was significantly higher than that for fragments, at  $p < 0.05$ , implying dominance of fibers in the tap water samples.

The overall fiber-count was found to be 55.0 p/L, comprising nearly 58% of the total particle count. Fragments (36.0 p/L) constituted 37%, with films (5.0 p/L) representing only 5%. Considering the total particle count per location, the samples from L<sub>1</sub> (80.0 p/L) and L<sub>2</sub> (92.0 p/L), which used a water filtration system (AQUA GUARD, AG-300, 2-column, carbon-resin) to filter the tap water at the point of usage, showed less contamination than the non-filtered tap water from L<sub>3</sub> (102.0 p/L), L<sub>4</sub> (101.0 p/L), and L<sub>5</sub> (104.0 p/L). The mean values of the size-based MP counts corresponding to L<sub>1</sub> and L<sub>2</sub> were significantly lower than those from the other locations. This is convincing evidence that the carbon-resin filtration facilitated MP reduction.

Size and shape are major particle characteristics that influence MP uptake and translocation after particles are ingested (Wright & Kelley [11]). McCullough, *et al.* [12] have reported that micro- and nano-particles cross the intestinal epithelial barrier into bodily fluids and other sites. Wu, *et al.* [13] have studied the size-dependent toxicity of MPs, focusing on the cellular uptake of polystyrene (PS) particles by human intestinal cells.

Urban, *et al.* [14] found that PE particles of up to 50  $\mu\text{m}$  translocate from lymph nodes to the liver and spleen, causing inflammatory and immune responses. The effects of the shape of polymeric carriers on the bio-distribution and cellular uptake are well described in encapsulation technology (Zheng & Yu [15]), which can be similarly applied to understand the susceptible shapes for cellular ingestion.

As per Zheng & Yu [15], smaller sized fibers and spherical shaped particles with less volume are easily engulfed by cells during phagocytosis. In addition, the

prevalence of polymeric microfibers in lung cancer tissue biopsies has provided evidence that MPs in the form of fibers lead to higher cellular uptake (Wright & Kelley [11]). Hence, the high amount of fibers in these tap water samples constitutes a potential risk if they are ingested at a high dose.

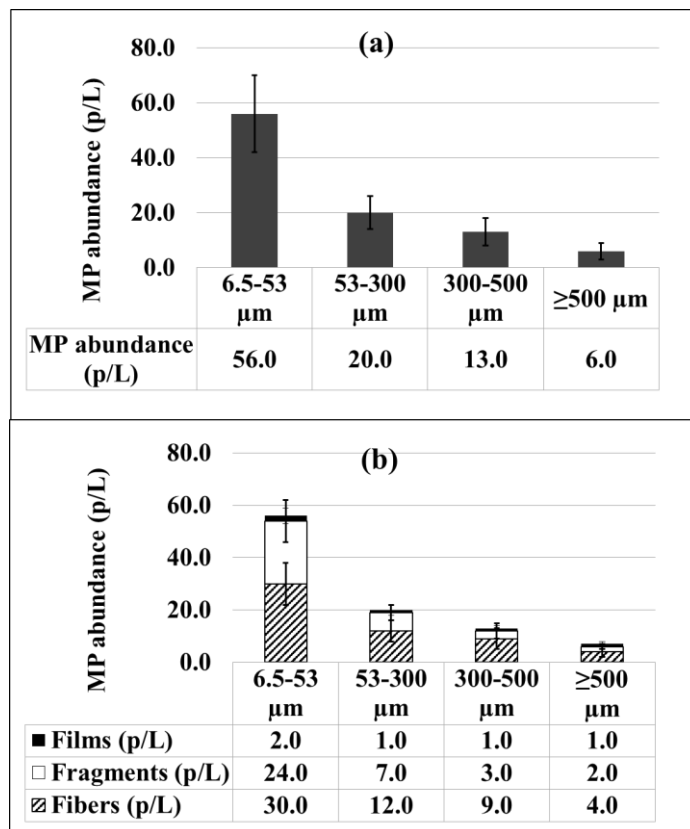


**Figure 3** Average MP count: a) size-based; b) morphology-based.

### 3.4 ATR-FT-IR Identification of $\geq 300$ $\mu\text{m}$ Particles

Figure 4 shows the ATR-FT-IR spectra of a) blue fibers b) red fibers, and c) transparent fibers observed under the optical microscope, showing critical absorption peaks corresponding to polyvinylchloride (PVC), PE, and PP, respectively. Most of the blue and bluish-transparent particles were confirmed to be polyethylene terephthalate (PET), while the white, brown, and red particles were identified as PE, and the transparent particles as PP. Usually, in the analysis of environmental samples, MP researchers use their color for the preliminary identification of polymer type. For instance, they ascribe transparent items to PP, white particles to PE, and other opaque colors to low-density polyethylene



(LDPE) (Rocha-Santos & Duarte [8]). In this study, the results of the FT-IR analysis support the above color-based attributes that were assigned to plastic particles for preliminary identification. The overall polymer distributions for 300-500  $\mu\text{m}$  and  $\geq 500 \mu\text{m}$  are shown in Table 2.

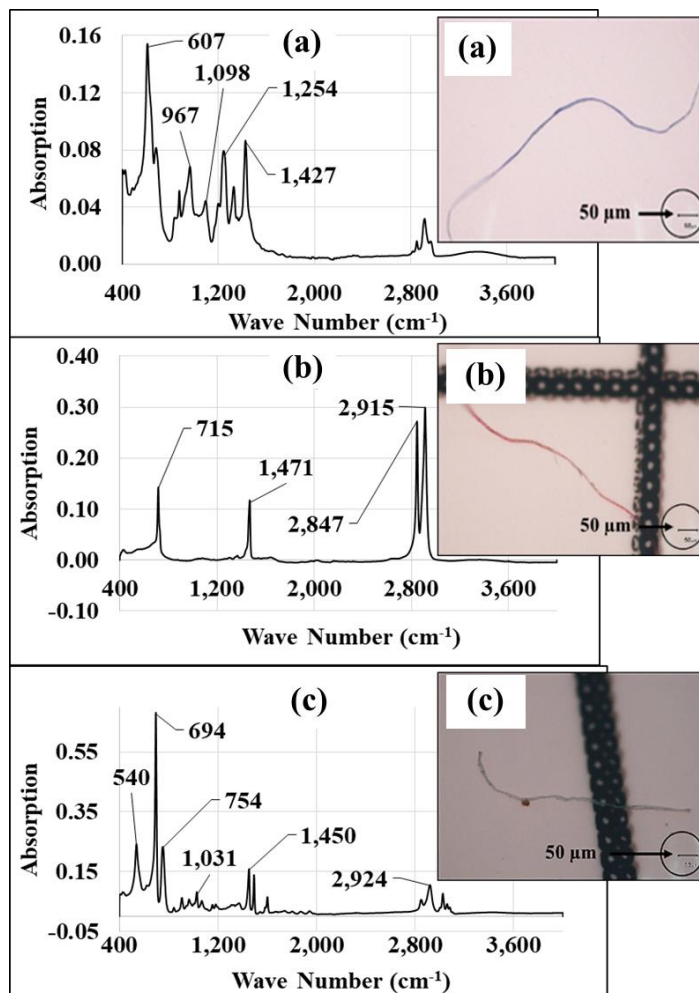


**Figure 4** ATR-FT-IR spectra of a) blue fibers: PVC; b) red fibers: PE; c) transparent fibers: PP.

Out of 590 particles sorted from the 300-500  $\mu\text{m}$  fraction, 272 were identified as polymeric particles, while 182 out of 279 particles were confirmed to be polymers in the  $\geq 500 \mu\text{m}$  fraction. This manual sorting and subsequent identification of MPs by FT-IR spectroscopy involves a bias. Therefore, Koelmans, *et al.* [16]

have recently put forward several criteria to ensure the reliable assessment of polymer identity in MP research. For drinking water, if the pre-sorted particle number is  $> 100$ , it is recommended to identify at least 50%, with a minimum of 100 particles (Koelmans, *et al.* [16]).

In this study, the number of pre-sorted particles was  $> 100$  for 300-500  $\mu\text{m}$  and  $\geq 500 \mu\text{m}$  particles. These two fractions were analyzed with 46.1% and 65.2% identification rates, respectively, detecting more than 100 particles in both instances. Hence, the aforementioned criteria were amply met in the FT-IR identification. In both distributions, PE was found to be dominant, representing 26.5% (300-500  $\mu\text{m}$ ) and 18.7% ( $\geq 500 \mu\text{m}$ ) of the total particles tested by spectroscopy. PVC was the second-highest component with 19.1% (300-500  $\mu\text{m}$ ) and 18.1% ( $\geq 500 \mu\text{m}$ ). PET, PA, PP, polyacrylamide (PAM), Teflon (PTFE), poly(methyl methacrylate) (PMMA), and PS were found in both size fractions. Apart from those, some  $\geq 500 \mu\text{m}$  particles were identified as cellophane and polybutadiene. The reason for the dominance of PE, PVC, and PA is the abrasion of pipes and fittings in drinking water treatment plants and the water supply network that runs from the distribution tanks to the households, which are mainly made of PVC, PE, and PA (Mintenig, *et al.* [16]). PET and other polymers are more likely to contaminate the raw water that enters the treatment plants.

The water for Thammasat University is supplied by a conventional water treatment plant that treats raw water from the Chao-Phraya River. A recent field study by Ericsson & Johansson [18] has shown MP pollution in the downstream Chao-Phraya River (Bangkok area), which is the prime entry-route of MPs into the treatment plant. There is a high possibility that those particles in the raw water are not entirely trapped by the treatment units and escape the plant along with the treated effluent. For example, PP and PS particles, which are relatively low-dense polymers, can easily escape with clarified water without undergoing sedimentation.

Recent findings on PET and PP in treated water samples from several plants by Pivokonsky, *et al.* [19] support this assumption. Moreover, PAM, an anionic polyelectrolyte, was added to the clarification tanks after the alum dosage to enable flocculation, suggesting that the PAM in the tap water had contaminated the water during the treatment process. In addition, given the signs of positive background contamination of PE, PP, and PA, certain particles could be added from atmospheric fall-out during sampling, processing, and analysis. Regarding PE-, PS-, and PP-MPs, Wu, *et al.* [13] and Schirinzi, *et al.* [20] have confirmed their potential for cellular uptake. Thus, the amount of PE that was found in this study constitutes a potential risk that humans are exposed to by consuming MP-contaminated water.

**Table 2** Polymer distribution for 300-500  $\mu\text{m}$  and  $\geq 500 \mu\text{m}$  fractions.

a) 300-500 $\mu\text{m}$ fraction		b) $\geq 500 \mu\text{m}$ fraction	
PE: 26.5%	PTFE: 5.9%	PE: 18.7%	PAM: 6.0%
PVC: 19.1%	PAM: 5.9%	PVC: 18.1%	PMMA: 4.9%
PET: 15.8%	PS: 5.1%	PA: 14.8%	Cellophane: 3.8%
PA: 10.3%	PMMA: 4.4%	PET: 13.7%	Polybutadiene: 3.3%
PP: 7.0%	-	PTFE: 7.1%	PS: 2.7%
-	-	PP: 6.6%	-

#### 4 Conclusions

All 45 tap water samples were found to contain particles of a polymeric nature, which were averaged across four size fractions: 6.5-53  $\mu\text{m}$  ( $56.0 \pm 14.0$  p/L) and 53-300  $\mu\text{m}$  ( $21.0 \pm 6.0$  p/L), sorted by Nile Red tagging; and 300-500  $\mu\text{m}$  ( $13.0 \pm 5.0$  p/L) and  $\geq 500 \mu\text{m}$  ( $6.0 \pm 3.0$  p/L) sorted by optical microscopy. These results show the significantly high amounts of MPs in the lower size fractions. Fibers were found in high amounts in all size categories, constituting 58% of the total count, followed by fragments and films.

From the ATR-FT-IR spectroscopy, PE, PVC, PET, PP, PTFE, PAM, and PA were mainly detected among the  $\geq 300 \mu\text{m}$  particles. They possibly originated from the treatment plant, following the water distribution process. MPs were found in tap water that was filtered by carbon-resin filters at the point of usage. This shows that particles still contaminate water, irrespective of filtration. With the past evidence provided on the cellular uptake of MPs it is vital to extend the study of MP concentrations in the water supply system. Subsequently, potential pathways and health implications can be correlated, while developing methods to mitigate contamination.

#### Acknowledgement

The authors would like to acknowledge the EFS scholarship grant from the Sirindhorn International Institute of Technology for this research.

#### References

- [1] Li, J., Liu, H. & Paul Chen, J., *Microplastics in Freshwater Systems: A Review on Occurrence, Environmental Effects, and Methods for Microplastics Detection*, Water Research, **137**, pp. 362-374, Jun 2018.
- [2] GESAMP, *Sources, Fate and Effects of Microplastics in the Marine Environment: Part Two of a Global Assessment*, Reports & Studies GESAMP No. 93, pp. 44-79, International Maritime Organization, London, 2016.

- [3] Ziajahromi, S., Neale, P.A., Rintoul, L. & Leusch, F.D.L., *Wastewater Treatment Plants as a Pathway for Microplastics: Development of a New Approach to Sample Wastewater-Based Microplastics*, Water Research, **112**, pp. 93-99, Apr 2017.
- [4] Kosuth, M., Mason, S.A. & Wattenberg, E.V., *Anthropogenic Contamination of Tap Water, Beer, and Sea Salt*, PLoS ONE, **13**(4), e0194970, Apr 2018.
- [5] Maes, T., Jessop, R., Wellner, N., Haupt, K. & Mayes, A.G., *A Rapid-Screening Approach to Detect and Quantify Microplastics Based on Fluorescent Tagging with Nile Red*, Scientific Reports, **7**, p. 44501, Mar 2017.
- [6] Erni-Cassola, G., Gibson, M.I., Thompson, R.C. & Christie-Oleza, J.A., *Lost, But Found with Nile Red: A Novel Method for Detecting and Quantifying Small Microplastics (1 mm to 20 µm) in Environmental Samples*, Environmental Science & Technology, **51**(23), pp. 13641-13648, Nov 2017.
- [7] Mason, S.A., Welch, V.G. & Neratko, J., *Synthetic Polymer Contamination in Bottled Water*, Frontiers in Chemistry, **6**, p. 407, Sep 2018.
- [8] Rocha-Santos, T.A.P. & Duarte, A.C., *Morphological and Physical Characteristics of Microplastics*, Wilson & Wilson's Comprehensive Analytical Chemistry: Characterization and Analysis of Microplastics, ed. 1, Rocha-Santos, T.A.P. & Duarte, A. C. (eds.), **75**, pp. 49-62, 2017.
- [9] Zhou, Q., Zhang, H., Fu, C., Zhou, Y., Dai, Z., Li, Y., Tu, C. & Luo, Y., *The Distribution and Morphology of Microplastics in Coastal Soils Adjacent to The Bohai Sea and The Yellow Sea*, Geoderma, **322**, pp. 201-208, Mar 2018.
- [10] Oßmann, B.E., Sarau, G., Holtmannspötter, H., Pischetsrieder, M., Christiansen, S.H. & Dicke, W., *Small-Sized Microplastics and Pigmented Particles in Bottled Mineral Water*, Water Research, **141**, pp. 307-316, Sep 2018.
- [11] Wright, S.L. & Kelley, F.J., *Plastic and Human Health: A Micro Issue?* Environmental Science & Technology, **51**(12), pp. 6634-6647, May 2017.
- [12] McCullough, M., Smyth, S.H., Moyes, S. & Carr, K.E., *Factors Influencing Intestinal Microparticle Uptake in Vivo*, International Journal of Pharmaceutics, **335**(1-2), pp. 79-89, May 2007.
- [13] Wu, B., Wu, X., Liu, S., Wang, Z. & Chen, L., *Size-Dependent Effects of Polystyrene Microplastics On Cytotoxicity and Efflux Pump Inhibition in Human Caco-2 Cells*, Chemosphere, **221**, pp. 333-341, Apr 2019.
- [14] Urban, R.M., Joshua, J., Jacobs, M.D., Michael, J. & Tomlinson, D.V.M., *Dissemination of Wear Particles to the Liver, Spleen and Abdominal Lymph Nodes of Patients with Hip or Knee Replacement*, The Journal of Bone and Joint Surgery, Incorporated, **82-A**, pp. 457-477, Apr 2000.

- [15] Zheng, M. & Yu, J., *The Effect of Particle Shape and Size on Cellular Uptake*, Drug Delivery & Translational Research, **6**(1), pp. 67-72, Feb 2016.
- [16] Koelmans, A.A., Nor, N.H.M., Hermesen, E., Kooi, M., Mintenig, S.M. & France, J.D., *Microplastics in Freshwaters and Drinking Water: Critical Review and Assessment of Data Quality*, Water Research, **155**, pp. 410-422, May 2019.
- [17] Mintenig, S.M., Loder, M. G.J., Primpke, S. & Gerdtts, G., *Low Numbers of Microplastics Detected in Drinking Water from Ground Water Sources*, Science of the Total Environment, **648**, pp. 631-635, Jan 2019.
- [18] Ericsson, E-H. & Johansson, E., *Quantification for the Flow of Microplastic Particles in Urban Environment: A Case of the Chao Phraya River, Bangkok, Thailand*, Degree Project in Technology, School of Architecture and the Built Environment, KTH Royal Institute of Technology, Stockholm, 2018.
- [19] Pivokonsky, M., Cermakova, L., Novotna, K. & Peer, P., *Occurrence of Microplastics in Raw and Treated Drinking Water*, Science of the Total Environment, **643**, pp. 1644-1651, Dec 2018.
- [20] Schirinzi, G. F., Perez-Pomeda, I., Sanchis, J., Rossini, C., Farre, M. & Barcelo, D., *Cytotoxic Effects of Commonly Used Nanomaterials and Microplastics on Cerebral and Epithelial Human Cells*, Environmental Research, **159**, pp. 579-587, Nov 2017.